Crystal Structure of the New Phosphate $AgMnPO_4$

Hamdi Ben Yahia, Etienne Gaudin, and Jacques Darriet

ICMCB, CNRS, Université Bordeaux 1, 87 Avenue du Docteur Schweitzer, 33608 Pessac Cedex, France

Reprint requests to H. Ben Yahia.
E-mail: benyahia.hamdi@uni-muenster.de

Z. Naturforsch. **2009**, *64b,* 875 – 878;
received May 6, 2009

The new compound $AgMnPO_4$ has been synthesized by a solid-state reaction route. Its crystal structure was determined from single-crystal X-ray diffraction data. $AgMnPO_4$ crystallizes with triclinic symmetry, space group $P\bar{1}$, a = 9.6710(6), b = 5.695(2), c = 6.629(3) Å, α = 102.55(3), β = 105.85(2), γ = 80.70(2)°, and Z = 4. Its structure is built up from MnO_6, MnO_5 and PO_4 polyhedra forming tunnels filled with silver atoms.

Key words: Phosphate, Single Crystal X-Ray Diffraction, Oxide

Introduction

Many compounds with the general formula $ABPO_4$ (A = alkali cation, Cu^+, Ag^+; B = alkaline earth cation, transition metal cation) were studied in the past. Theses phosphates crystallize mainly with four different structure types, *i. e*. olivine, maricite, stuffed-tridymite, or zeolite-ABW. The stuffed-tridymite or zeolite-ABW structure types are observed with the large alkali metals K, Rb or Cs located in the channels and acting as templates. In these structures the transition metal atoms are located in tetrahedral sites, but sometimes also in trigonal bipyramids. In the more condensed phases with olivine- or maricite-type structures the transition metal atoms are located in octahedral sites. We were interested to compare the structural evolution between homologous phosphates and vanadates, and for this the series $AMnPO_4$ and $AMnVO_4$ have been chosen. In the $AMnPO_4$ phosphate series, $LiMnPO_4$ [1], $NaMnPO_4$ [2], $KMnPO_4$ [3], and $CsMnPO_4$ [4] were studied in the past and their structures determined. Recently we have reported on the structural and magnetic characterization of $RbMnPO_4$ [5]. In the case of the

Table 1. Crystallographic data and structure refinement for $AgMnPO_4$.

Formula	$AgMnPO_4$
Crystal color	yellow block
Crystal size, mm^3	$0.060 \times 0.036 \times 0.026$
M, g mol^{-1}	257.8
Crystal system	triclinic
Space group	$P\bar{1}$
a, Å	9.6710(6)
b, Å	5.695(2)
c, Å	6.629(3)
α, deg	102.55(3)
β, deg	105.85(2)
γ, deg	80.70(2)
V, $Å^3$	340.8(2)
Z	4
$D_{calcd.}$, g cm^{-3}	5.02
T, K	293(1)
$F(000)$, e	476
Radiation; λ, Å	MoK_α; 0.71069
Monochromator	oriented graphite
$h\ k\ l$ range	$-8 \le h \le 9$; $-9 \le k \le 10$; $-15 \le l \le 13$
θ_{max}, deg	35
μ(MoK_α), mm^{-1}	9.8
T_{min} / T_{max}	0.655 / 0.795
No. of measured reflections	8775
No. of indep. reflections / R_{int}	1954 / 0.072
Reflections used with $I \ge 2\sigma(I)$	1556
Refinement	F^2
No. of refined parameters	128
R factors $R(F)$ / $wR(F^2)$	0.0323 / 0.0697
GoF	1.11
Weighting scheme	$w = 1/(\sigma^2(I) + 0.0009I^2)$
$\Delta\rho_{fin}$ (min/max), e $Å^{-3}$	−1.11 / +0.92

Table 2. Atom positions and equivalent displacement parameters ($Å^2$) for $AgMnPO_4$.

Atom	x	y	z	U_{eq} ($Å^2$)
Ag1	0.11744(5)	0.31332(7)	0.36952(6)	0.02101(14)
Ag2	0.24721(5)	0.83191(7)	0.48229(6)	0.02227(15)
Mn1	0.42628(8)	0.21824(11)	0.16773(11)	0.0079(2)
Mn2	0.21227(8)	0.66287(11)	0.93703(11)	0.0087(2)
P1	0.46136(12)	0.31231(17)	0.70882(17)	0.0057(3)
P2	0.08701(13)	0.18418(18)	0.84675(18)	0.0068(3)
O1	0.4420(3)	0.1287(5)	0.8360(5)	0.0097(10)
O2	0.6243(3)	0.3492(5)	0.7643(5)	0.0106(10)
O3	0.4014(4)	0.2270(5)	0.4726(5)	0.0120(11)
O4	0.3873(3)	0.5670(5)	0.7817(5)	0.0094(10)
O5	0.1983(4)	0.2281(6)	0.0631(5)	0.0172(11)
O6	0.9337(4)	0.2186(5)	0.8731(5)	0.0119(10)
O7	0.1210(4)	0.9229(5)	0.7338(5)	0.0129(11)
O8	0.1039(4)	0.3708(5)	0.7177(5)	0.0127(11)

Table 3. Anisotropic displacement parameters (Å^2) for $AgMnPO_4$. The anisotropic displacement factor exponent takes the form: $-2\pi^2[(ha^*)^2 U_{11} + \ldots + 2hka^* \cdot b^* U_{12}]$.

Atom	U_{11}	U_{22}	U_{33}	U_{12}	U_{13}	U_{23}
Ag1	0.0164(2)	0.0348(2)	0.0117(2)	0.00138(16)	0.00581(16)	0.00410(16)
Ag2	0.0188(2)	0.0350(2)	0.0123(2)	0.00373(16)	0.00843(16)	0.00205(16)
Mn1	0.0080(4)	0.0086(3)	0.0072(3)	−0.0007(2)	0.0024(3)	0.0014(2)
Mn2	0.0061(4)	0.0110(3)	0.0082(3)	0.0006(2)	0.0021(3)	0.0005(2)
P1	0.0056(6)	0.0068(4)	0.0045(5)	0.0001(4)	0.0012(4)	0.0009(4)
P2	0.0062(6)	0.0078(4)	0.0058(5)	−0.0012(4)	0.0015(4)	−0.0001(4)
O1	0.0133(18)	0.0068(12)	0.0109(15)	0.0006(11)	0.0053(13)	0.0040(11)
O2	0.0059(17)	0.0179(15)	0.0079(15)	−0.0036(12)	0.0009(13)	0.0015(12)
O3	0.0148(19)	0.0143(14)	0.0063(15)	−0.0025(12)	0.0023(13)	0.0004(12)
O4	0.0107(17)	0.0090(13)	0.0090(15)	0.0008(11)	0.0039(13)	0.0022(11)
O5	0.0088(18)	0.0336(18)	0.0068(15)	−0.0035(14)	0.0010(13)	−0.0008(14)
O6	0.0078(17)	0.0171(14)	0.0099(15)	−0.0018(12)	0.0026(13)	−0.0002(12)
O7	0.0165(19)	0.0113(13)	0.0124(16)	−0.0002(12)	0.0077(14)	0.0014(12)
O8	0.0177(19)	0.0096(13)	0.0129(16)	−0.0010(12)	0.0062(14)	0.0033(12)

analogous AMnVO$_4$ vanadates only LiMnVO$_4$ was known [6]. This compound crystallizes with the Na_2CrO_4-type structure, whereas LiFePO$_4$ crystallizes with the olivine type. Therefore, contrary to LiFePO$_4$, this compound is not of interest as a cathode material for rechargeable Li ion batteries [7].

Recently we have extended the AMnVO$_4$ vanadate series with AgMnVO$_4$ [8], CuMnVO$_4$ [9], KMnVO$_4$ [10], and RbMnVO$_4$ [8]. AgMnVO$_4$ crystallizes with the maricite-type structure and contains $[MnO_4]_\infty$ chains made up of edge-sharing MnO_6 octahedra. CuMnVO$_4$ crystallizes with the Na_2CrO_4 structure, similar to LiMnVO$_4$, and contains also $[MnO_4]_\infty$ chains made up of edge-sharing MnO_6 octahedra. Antiferromagnetic interactions in and between the chains have been detected. A surprising result was observed for KMnVO$_4$. Indeed, this compound crystallizes with a new type of oxygen-deficient perovskite structure. Antiferromagnetic interactions between the Mn^{2+} ions were observed. RbMnVO$_4$ is to our knowledge the first vanadate crystallizing with the stuffed tridymite-type structure. It exhibits canted antiferromagnetism [8].

To complete the AMnPO$_4$ series, we have synthesized the new compound AgMnPO$_4$ and studied its structure.

Experimental Section

Synthesis

Powder samples of AgMnPO$_4$ were prepared by direct solid-state reaction from stoichiometric mixtures of Ag_2O, MnO and $(NH_4)H_2PO_4$ powders. The mixtures were ground in an agate mortar and heated at 500 °C for 12 h in a gold crucible under an argon atmosphere. The resulting powders were ground and fired at 700 °C for several days with intermediate grinding. The progress of the reactions was followed by powder X-ray diffraction. The powder sample was not pure.

Table 4. Interatomic distances (in Å) and bond valences (B. V.) for AgMnPO$_4$. Average distances are given in brackets.

	Distance	B. V.		Distance	B. V.
Ag1–O8	2.297(3)	0.292	Mn1–O3	2.089(3)	0.446
Ag1–O5	2.300(4)	0.29	Mn1–O5	2.118(3)	0.412
Ag1–O8	2.585(3)	0.134	Mn1–O1	2.170(3)	0.358
Ag1–O3	2.634(3)	0.118	Mn1–O1	2.188(3)	0.341
Ag1–O7	2.708(4)	0.096	Mn1–O4	2.250(3)	0.288
		0.930[a]	Mn1–O2	2.400(3)	0.192
Ag2–O7	2.252(4)	0.330		⟨2.203⟩	2.037[a]
Ag2–O2	2.290(3)	0.298	Mn2–O6	2.080(4)	0.457
Ag2–O6	2.512(3)	0.164	Mn2–O7	2.141(3)	0.387
Ag2–O4	2.688(3)	0.102	Mn2–O4	2.152(3)	0.376
Ag2–O3	2.914(4)	0.055	Mn2–O8	2.158(3)	0.370
Ag2–O1	2.966(3)	0.048	Mn2–O2	2.176(3)	0.352
		0.997[a]		⟨2.141⟩	1.942[a]
P1–O3	1.513(3)	1.325	P2–O6	1.517(4)	1.310
P1–O1	1.540(4)	1.231	P2–O5	1.538(3)	1.238
P1–O4	1.549(3)	1.202	P2–O7	1.541(3)	1.228
P1–O2	1.556(3)	1.179	P2–O8	1.554(4)	1.186
	⟨1.540⟩	4.937[a]		⟨1.538⟩	4.962[a]

[a] Bond valence sum (B. V.) = $e^{(r^0-r)/b}$ with the following parameters: b = 0.37, r_0 (Ag^I–O) = 1.805, r_0 (P^V–O) = 1.604 and r_0 (Mn^{II}–O) = 1.790 Å [16, 17].

Various other attempts to synthesis a pure sample were also unsuccessful. Single crystals were then prepared by heating the stoichiometric mixture at 950 °C for 1 h and cooling it slowly at a rate of 5 °C h^{-1} to ambient temperature. Single crystals of AgMnPO$_4$, $Mn_2P_2O_7$ and Ag_2O were identified in the sample.

X-Ray diffraction

Single crystals of AgMnPO$_4$ suitable for X-ray diffraction were selected on the basis of the size and the sharpness of the diffraction spots. The data collection was carried out on an Enraf-Nonius Kappa CCD diffractometer using MoK_α radiation. Data processing and all refinements were performed with the JANA2006 program package [11]. A Gaussian-type absorption correction was applied, and the crystal shape was

determined with the video microscope of the Kappa CCD. For data collection details, see Table 1.

Structure refinement

The structure of $AgMnPO_4$ was refined in the space group $P\bar{1}$. The starting atomic positions were those reported for the isotypic compound $AgCoPO_4$ [12]. With anisotropic displacement parameters applied to all positions, the final residual factors converged to the values given in Table 1. The refined atomic positions and anisotropic displacement parameters are listed in Tables 2 and 3, respectively.

Further details of the crystal structure investigation may be obtained from Fachinformationszentrum Karlsruhe, 76344 Eggenstein-Leopoldshafen, Germany (fax: +49-7247-808-666; e-mail: crysdata@fiz-karlsruhe.de, http://www.fiz-informationsdienste.de/en/DB/icsd/depot_anforderung.html) on quoting the deposition number CSD-420703.

Discussion

The structure of $AgMnPO_4$ is based on an ordered three-dimensional framework of MnO_6, MnO_5 and PO_4 polyhedra that forms channels parallel to the crystallographic *b* axis, and into which the Ag atoms are stuffed (Fig. 1). The $Mn1O_6$ octahedra and the $Mn2O_5$ trigonal bipyramids are connected by sharing corners to four and five PO_4 tetrahedra, respectively (Fig. 2). Two $Mn1O_6$ octahedra are sharing the O1–O1 edge

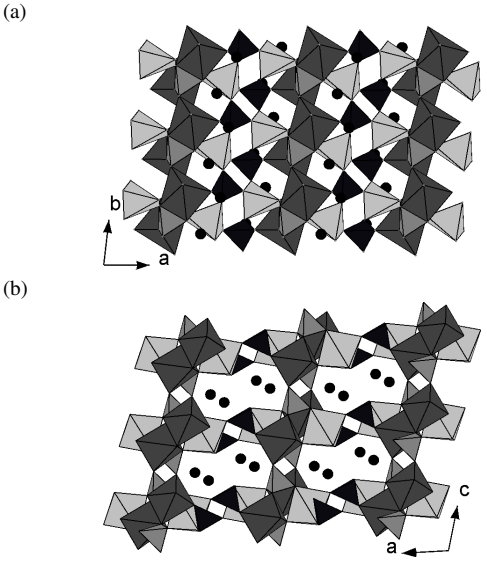

Fig. 1. View of the $AgMnPO_4$ structure along (001) (a), and (010) (b). The light grey, medium grey, dark grey and black polyhedra correspond to $Mn2O_5$, $P1O_4$, $Mn1O_6$ and $P2O_4$ polyhedra. The silver atoms are displayed with black spheres.

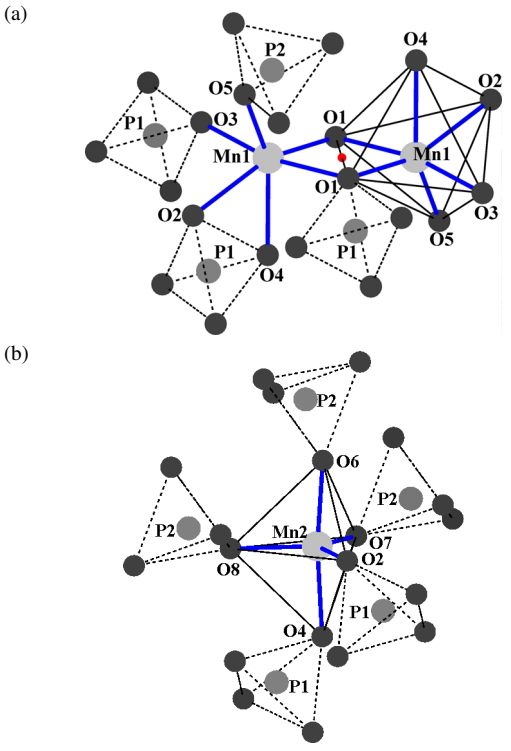

Fig. 2. Environment of the $Mn1O_6$ (a) and $Mn2O_5$ (b) polyhedra. The point drawn in the middle of the O1–O1 edge corresponds to the inversion center.

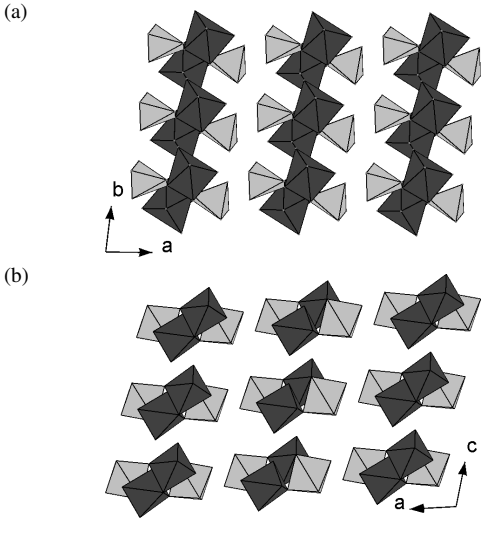

Fig. 3. View of the building units induced from the connection of the Mn1 dimers through Mn2 bipyramids along [001] (a) and [010] (b).

and form a $(Mn1)_2O_9$ unit. The two octahedra are related by an inversion center (Fig. 2a). The $(Mn1)_2O_9$

dimers are connected through $Mn2O_5$ bipyramids to form ribbons running parallel to the *b* axis (Figs. 3a and 3b). The PO_4 tetrahedra connect these ribbons to form a three-dimensional network giving rise to channels along the *b* axis, where the silver ions are located. The interatomic distances Ag–O, Mn–O and P–O are listed in Table 4.

The PO_4 tetrahedra are quite regular with an average distance of 1.540 and 1.538 Å for P1 and P2, respectively. This is consistent with the value of 1.55 Å estimated from the effective ionic radii of the four-coordinated P^{5+} and O^{2-} ions [13]. In the distorted $Mn1O_6$ octahedra, the distances range from 2.089 to 2.400 Å with an average value of 2.203 Å, whereas in the $Mn2O_5$ bipyramids the distances range from 2.080 to 2.176 Å with an average distance of 2.141 Å. Such a five-coordinated Mn^{2+} environment occurs also in $Mn_3P_2O_8$ [14] with distances ranging from 2.086 to 2.168 Å and an average distance of 2.139 Å, in good agreement with our results. The coordination polyhedra of the silver ions are not well defined. The Ag–O distances cover the large range from 2.297 to 2.708 Å and from 2.252 to 2.966 Å for the five- and six-coordinated Ag1 and Ag2 atoms, respectively. The short Ag1–Ag2 distance of 2.988 Å is close to the one observed in $AgCoPO_4$ (2.945 Å) and slightly larger than the one observed in metallic silver, (2.889 Å). Such short Ag–Ag distances (d^{10}-d^{10} interactions) were also observed in many other compounds listed by Jansen [15]. The results of the bond valence sum calculations (Table 4) [16] confirmed the expected charge balance $Ag^{I}Mn^{II}P^{V}O_4{}^{-II}$.

[1] S. Geller, J. L. Durand, *Acta Crystallogr.* **1960**, *13*, 325 – 331.
[2] J. Moring, E. Kostiner, *J. Solid State Chem.* **1986**, *61*, 379 – 383.
[3] M. Lujan, F. Kubel, H. Schmid, *Z. Naturforsch.* **1995**, *50b*, 1210 – 1214.
[4] O. V. Yakubovich, M. A. Simonov, O. K. Mel'nikov, *Kristallografiya* **1990**, *35*, 42 – 46.
[5] H. Ben Yahia, E. Gaudin, J. Darriet, *J. Alloys Compd.* **2007**, *442*, 74 – 76.
[6] A. K. Padhi, W. B. Archibald, K. S. Nanjundaswamy, J. B. Goodenough, *Solid State Chem.* **1997**, *128*, 267 – 272.
[7] S.-Y. Chung, J. T. Bloking, Y.-M. Chiang, *Nature Mater.* **2002**, *1*, 123 – 128.
[8] H. B. Yahia, E. Gaudin, J. Darriet, *J. Solid State Chem.* **2008**, *181*, 3103 – 3109.
[9] H. B. Yahia, E. Gaudin, J. Darriet, M. Banks, R. K. Kremer, A. Villesuzanne, M. H. Whangbo, *Inorg. Chem.* **2005**, *44*, 3087 – 3093.
[10] H. Ben Yahia, E. Gaudin, C. Lee, M. H. Whangbo, J. Darriet, *Chem. Mater.* **2007**, *19*, 5563 – 5569.
[11] V. Petříček, M. Dušek, L. Palatinus, JANA2006, The Crystallographic Computing System, Institute of Physics, University of Prague, Prague (Czech Republic) **2006**.
[12] I. Tordjman, J. C. Guitel, A. Durif, M. T. Averbuch, R. Masse, *Mater. Res. Bull.* **1978**, *13*, 983 – 988.
[13] R. D. Shannon, *Acta Crystallogr.* **1976**, *A32*, 751 – 767.
[14] B. El Bali, A. Boukhari, R. Glaum, M. Gerk, K. Maass, *Z. Anorg. Allg. Chem.* **2000**, *626*, 2557 – 2562.
[15] M. Jansen, *Angew. Chem.* **1987**, *99*, 1136 – 1149; *Angew. Chem., Int. Ed. Engl.* **1987**, *26*, 1098 – 1110.
[16] I. D. Brown, D. Altermatt, *Acta Crystallogr.* **1985**, *B41*, 244 – 247.
[17] N. E. Brese, M. O'Keeffe, *Acta Crystallogr.* **1991**, *B47*, 192 – 197.